

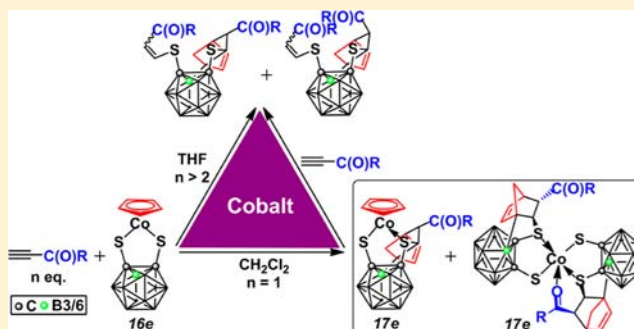
Unprecedented Boron-Functionalized Carborane Derivatives by Facile and Selective Cobalt-Induced B–H Activation

Zhaojin Wang, Hongde Ye, Yuguang Li, Yizhi Li, and Hong Yan*

State Key Laboratory of Coordination Chemistry, School of Chemistry and Chemical Engineering, Nanjing University, Nanjing, Jiangsu 210093, China

S Supporting Information

ABSTRACT: The 16-electron complex $\text{CpCoS}_2\text{C}_2\text{B}_{10}\text{H}_{10}$ (**1**) is found to react with the alkynes $\text{HC}\equiv\text{CC}(\text{O})\text{R}$ [R = methyl (Me), phenyl (Ph), styryl (St), ferrocenyl (Fc)] at ambient temperature to give two types of 17-electron cobalt complexes **2a–d** and **3a–d** containing unique B(3)/B(6)-norbornyl carborane moieties. A formation mechanism via a tandem sequence of metal-induced B–H activation, B–Cp formation, Cp delivery and Diels–Alder addition is proposed on the basis of DFT calculations. The reactivity of these paramagnetic 17-electron complexes has been studied: Exposed to a combination of air, moisture and silica, complexes **2a–d** undergo alkyl C–S cleavage to give 16-electron complexes **4a–c** containing a boron-norbornadienyl moiety, and simultaneous carboranyl C–S cleavage to afford cobalt-free carborane derivatives **5a–d** containing a boron-norbornyl unit. Both **2a–d** and **3a–d** allow further alkyne insertion into the Co–S bond to generate cobalt-free boron–norbornyl carborane derivatives (*Z/E*)-**7a–d** and (*Z/E*)-**8a–d**, both containing a vinyl sulfido group. Addition of AlCl_3 not only promotes the conversion of **2a–d**, but also leads predominantly to (*E*)-**9a–d** as retro-Diels–Alder products. Upon heating, the isomerization from *E* to *Z*-configuration of the vinyl group and reorganization of the norbornyl moiety of (*Z/E*)-**7a–d** occur to lead to (*Z*)-**9a–d** as well as the unexpected [1,2]-H shifted products (*Z*)-**10b,c**. Thus, the 17-electron complexes **2a–d** and **3a–d** serve as intermediates for synthesis of variety of boron-functionalized carborane derivatives. In this study, efficient routes have been developed through cobalt-mediated B–H activation to prepare boron-functionalized carborane derivatives that are unavailable by conventional routes.



INTRODUCTION

Dicarba-*closo*-dodecaboranes (*o*-, *m*-, and *p*-carboranes) have been used for decades as versatile building blocks for construction of functional materials and pharmaceuticals^{1–3} because of their useful properties such as thermal stability, unique structures and electronic effects, enriched boron content and low biotoxicity. To enable those diverse applications, structural modifications of carboranes have been the first concern. Substitution in the carbon positions was readily achieved via deprotonation of C–H as early as the discovery of carboranes in 1960s. Substitution at the boron atoms, however, remains less explored because of the less acidic B–H bonds.^{3f,4} In particular, selective boron-functionalization of carborane clusters is still a synthetic challenge because of the chemically close B–H bonds and limited functional groups.⁵ This situation seriously restricts further development of applications of carborane derivatives. Until now boron-substitution of *o*-carborane was mainly accomplished by electrophilic substitution to give, for example, boron-alkylation,⁶ boron-halogen⁷ and boron-chalcogen,⁸ but the reactive sites of these examples were mostly localized on B(9)/B(12), which is attributed to the inherent charge distribution of the *o*-carborane cage.⁹ Substitution in the alternative B(3)/B(6) positions suffered

from a major restriction that the key starting material 3-iodo-*o*-carborane was typically synthesized by deboronation (using a base) to form *nido*-carborane, followed by cage reconstruction using BI_3 , thus limiting options for further substitution in these two positions.¹⁰ Moreover, metal-promoted selective boron-substitution has proven difficult although significant advances have been achieved,^{11–14} among which boron-functionalization by organic groups was rare.^{13,14}

Selective B–M ($\text{M} = \text{Rh}, \text{Ir}, \text{Ru}, \text{Os}$) and B–C (B-alkyl and B-vinyl) formation via intramolecular metal-induced *o*-carborane B(3)/B(6)–H activation has been reported.¹⁵ Recent advances in cobalt-induced B–H/C–H activation leading to B–C coupling and cobalt-bound-Cp (Cp = cyclopentadienyl) involved Diels–Alder reaction leading to boron-norbornyl formation have brought renewed interest.^{16,17} Of these examples, the formation of unprecedented boron-norbornyl group observed in the reaction of $\text{CpCoS}_2\text{C}_2\text{B}_{10}\text{H}_{10}$ and $\text{HC}\equiv\text{CC}(\text{O})\text{Ph}$ appeared far from a conventional route,¹⁷ therefore inspiring us to make further exploration. In this study we have extended the scope of alkynes, investigated the complicated

Received: May 10, 2013

Published: July 8, 2013

mechanism by theoretical calculations and examined the reactivity that has led to synthesis of numerous boron-functionalized carborane derivatives. The in-depth study demonstrates the feasibility of cobalt-induced selective B–H functionalization that can provide a variety of boron-functionalized carborane derivatives bearing in situ generated norbornyl or norbornadienyl functional group.

RESULTS AND DISCUSSION

1. Synthesis and Characterization of 17-Electron Complexes 2a–d and 3a–d. The reactions of $\text{CpCoS}_2\text{C}_2\text{B}_{10}\text{H}_{10}$ (**1**) and selected four alkynes $\text{HC}\equiv\text{CC}(\text{O})\text{R}$ ($\text{R} = \text{Me}, \text{Ph}, \text{St}, \text{Fc}$) at ambient temperature led to two types of 17e complexes **2a–d** and **3a–d** with combined isolated yields 40–50% based on complex **1** (Scheme 1).

Scheme 1. Synthesis of **2a–d** and **3a–d**



The single crystal structure of **2a** (Figure 1a) shows a new-generated norbornyl moiety that combines to the starting 16e complex **1** through both C–S and B–C bonds. The norbornyl unit that bears *endo* configuration¹⁸ appears to be constructed by the original alkyne (blue) and Cp (red) (Scheme 1). The acetyl group and S(2) are in *anti*-arrangement with respect to C(3)–C(4) bond. As one Co–S bond has been changed to a coordinating $\text{Co} \leftarrow \text{S}$ bond, complex **2a** acts as a 17e species, and the cobalt center is in a formal charge of +2. The paramagnetic characteristic of species **2a–d** are indicated by NMR data as shown by the broad signals (15 to –10 ppm for ¹H NMR and 20 to –30 ppm for ¹¹B NMR) that could not be accurately identified (Supporting Information (SI), Figures S3.1/2). Crystal structure of **3b** (Figure 1b) shows the cobalt center is bound to two B(3)/B(6)-norbornyl carborane units through $\text{Co} \leftarrow \text{S}$ and $\text{Co}-\text{S}$ bonds as in **2a**. The core geometry of **3b** exhibits distorted trigonal bipyramid in which S(2)/S(4) are located above/below S(1)–O(1)–S(3) plane, and the angle between Co(1)–S(1)–S(2) and Co(1)–S(3)–S(4) planes is 61.8°, in sharp contrast to the known planar cobaltadithiolene complexes.¹⁹ Unlike **2a**, the Co–S distances in **3b** are significantly different with Co–S 2.25 Å and $\text{Co} \leftarrow \text{S}$ 2.50 Å. Because of the oxygen-coordination to cobalt, the benzoyl group in the substituted norbornyl moiety takes *syn*-arrangement with S(2), whereas the other benzoyl adopts *anti*-arrangement with S(4), the same as in **2a**. In view of the structure of **3b**, it appears to be a combination of two molecules of **2b** with loss of a Cp_2Co fragment. The electron count of cobalt in **3b** is also 17 with cobalt in formal charge of +2. In contrast to **2a–d**, the effect of paramagnetism of **3a–d** on NMR is much larger; for example, the signals span from 100 to –15 ppm for ¹H NMR and from 300 to –20 ppm for ¹¹B NMR (SI, Figures S3.3/4).

As implied by the solid-state structures of complexes **2a** and **3b**, sequential steps such as B–H activation and Cp-participated Diels–Alder addition must be involved in their

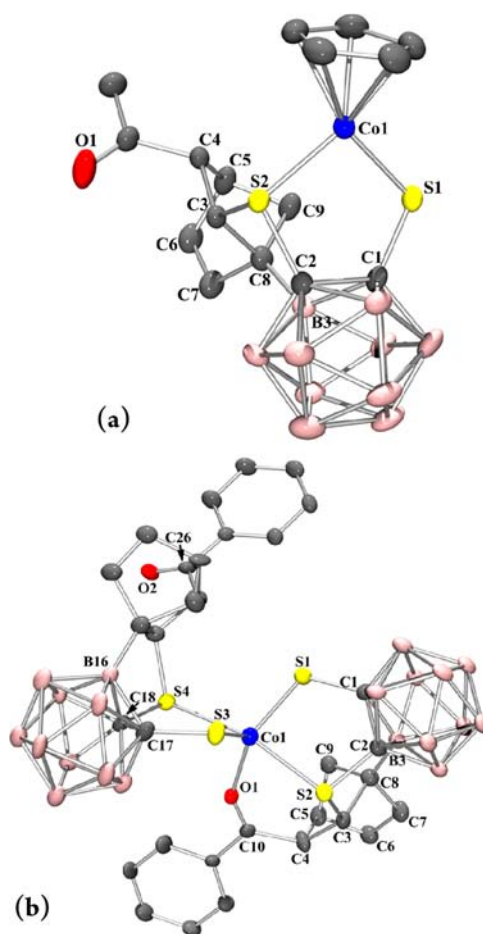


Figure 1. Crystal structures of **2a** (a) and **3b** (b). Selected bond lengths [Å] and angles [°]: **2a**, Co1–S1 2.1563(6), Co1–S2 2.1762(6), C1–S1 1.785(2), C2–S2 1.807(2), C3–S2 1.864(2), C1–C2 1.663(3), C3–C4 1.528(3), C6–C7 1.314(4), C8–B3 1.570(3); **3b**, Co1–O1 2.036(2), Co1–S1 2.2461(1), Co1–S2 2.5499(9), Co1–S3 2.2423(1), Co1–S4 2.4577(9), C10–O1 1.215(4), C26–O2 1.200(4); S1–Co1–S2 89.97(3), S3–Co1–S4 90.78(3).

formation. Even though metal-bound Cp were reactive in many reactions,²⁰ including in Diels–Alder addition,²¹ its intramolecular combination with olefinic unit and substitution at B(3)/B(6) site of carborane could be only observed in few examples contributed by our group.^{16,17}

2. Formation Mechanisms of 2a–d and 3a–d: A DFT Study. Complexes **2a–d** and **3a–d** are unique; thus, mechanistic study is essential to better understand their formation processes. However, elucidation of the formation mechanism by routine analytical means such as NMR and MS is not realistic because of the complicated reaction mixture along with paramagnetic disturbance (SI, S.1). Therefore, theoretical calculations in combination of experimental evidence were utilized to demonstrate the mechanistic processes. DFT calculations on the formation of **2a** were conducted using the um06²²/6-31g(d, p) basis set for all noncobalt atoms and lan12dz²³ for cobalt, as is a common treatment for this class of organometallic complexes.²⁴ The calculated energy profile is shown in Figure 2.

The sequence starts from alkyne insertion into a Co–S bond via a concerted transition state (**TS₁**, energy barrier 14.5 kcal/mol) and is favored by –9.3 kcal/mol energy change leading to

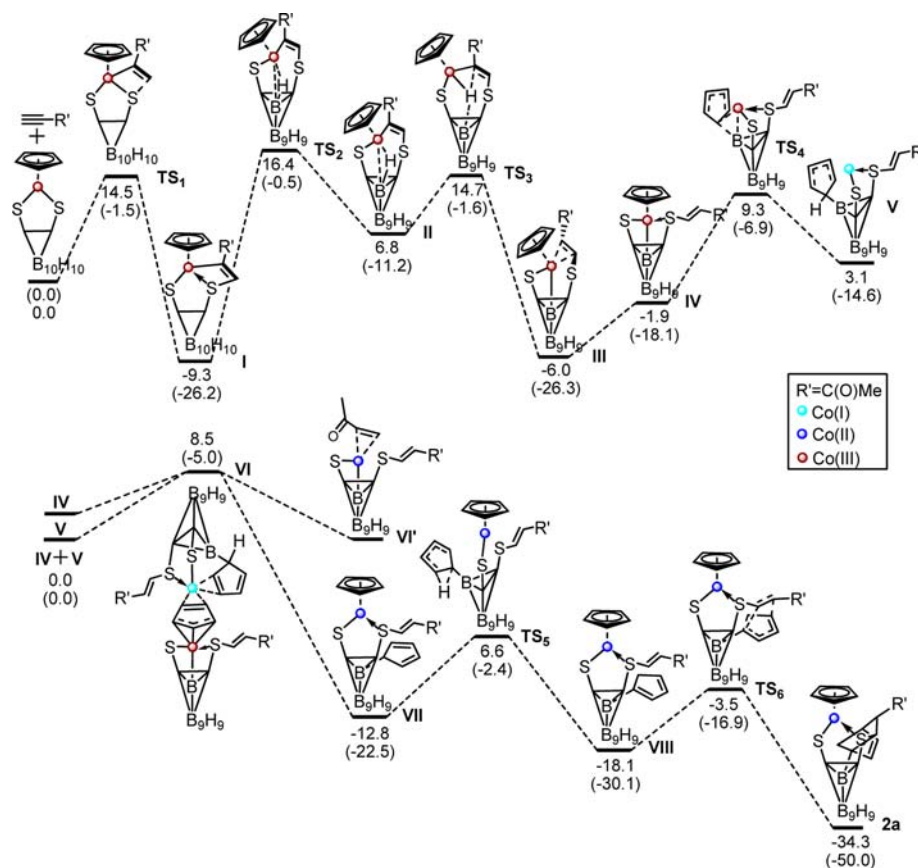


Figure 2. Energy profile for 2a formation. The relative free energy and the electronic energy (in the bracket) for each intermediate or transition state are given in kcal/mol.

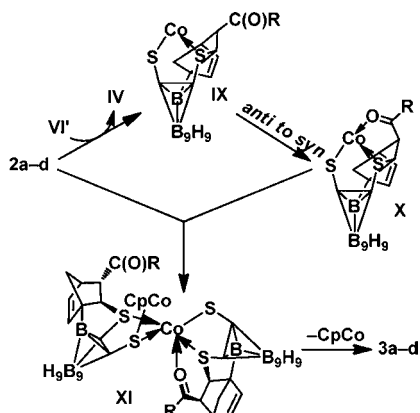
intermediate I (see an isolated analogue generated from **1** and MeO₂CC≡CCO₂Me).²⁵ In the following step, the CpCo group is reoriented (via TS₂, energy barrier 25.7 kcal/mol) to give a B–H σ complex II with an energy demand of 16.1 kcal/mol. In II, typical stabilization of B–H σ bond to Co (LP*, anti-bond orbital of Lewis pair) is calculated as 43.2 kcal/mol from natural bonding orbitals (NBO) analysis.²⁶ This σ -coordination leads to the B–H bond weakening, as indicated by a longer B(3)–H bond (1.24 vs 1.18 Å in I, SI, Figure S6.2.2). The B–H activation that further leads to hydrogen transfer from B(3) to vinyl is an energy-favored process ($\Delta G = -12.8$ kcal/mol), whereas the transition state (TS₃, energy barrier 7.9 kcal/mol) that connects II and III is located as a Co–H structure in which the B(3)⋯H distance is 1.54 Å.

The structure of III has two notable features, i.e., Co–B bond, which is optimized as 2.03 Å (referred to 2.01 Å in one related example¹⁵ⁱ), and vinyl coordination to cobalt. Similar complexes with a M–B bond (M = Rh, Ir, Ru, Os)^{15b,d,27} were sufficiently stable to allow isolation and even characterization by X-ray crystallography. However, III can easily convert to IV by vinyl stretch with energy consumption of 4.1 kcal/mol. In the optimized structure of IV, the shortest distance between C(η^5 -Cp) and B(3) is 2.81 Å, thus allowing B–Cp²⁸ formation (V) through reductive elimination, as the energy barrier (TS₄, Co⋯B⋯C²⁹ transition structure) for this step is only 11.2 kcal/mol. Within V, cobalt is coordinated by Cp (neutral) in η^4 -mode with +1 valence state. Note that TEMPO (2,2,6,6-tetramethyl-1-piperidinyloxy) inhibited the reaction, which may oxidize this Co(I) species (SI, S.2).

Starting from V, the involvement of C₃H₅⁻ or Cp• was empirically excluded because of very high energy activation (SI, 6.3). The direct Cp delivery between IV and V supplies the required C₃H₅ unit, and intermediate VI was located (only 8.5 kcal/mol above IV and V) in which IV and V share one Cp ligand, similar to many triple-decker complexes.³⁰ The Cp ligand combines to Co(III)/Co(I) in η^3/η^2 modes simultaneously, and each cobalt in VI possesses 16 electrons. Thereafter, through η^3 -Cp dissociation and electron transfer, the smooth formation of Co(II) intermediates VI' and VII occurs with 21.3 kcal/mol energy lowering. Next, [1,5]-H shift³¹ from VII to VIII occurs and releases 5.3 kcal/mol energy, by overcoming a 19.4 kcal/mol barrier (TS₅). The Diels–Alder process that leads to the final boron-norbornyl moiety in 2a proceeds smoothly from VIII with further energy lowering of 16.2 kcal/mol. Hence these results deduce an interesting sequence: the cobalt-induced B–H activation leads to reactive Co–B species IV, which rationalizes the key combination of carboranyl and cyclopentadienyl units, thus supplying an appropriate platform for boron-norbornyl formation in 2a.

The formation of 3a–d follows from 2a–d as the boron-norbornyl moiety should be established prior to the bipyramidal core geometry. However, no direct conversion from isolated 2a–d to 3a–d was experimentally observed, implying that an in situ generated mediator is involved. Since intermediate VI' exhibits severe coordination unsaturation on cobalt, Cp might deliver from 2a–d to VI' to lead to intermediates IV and IX (Scheme 2). To compensate electron shortage in IX, the carbonyl group is driven to coordinate to

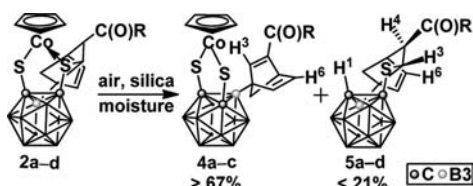
Scheme 2. Proposed Formation Mechanism of 3a–d



cobalt (X). The further combination of X with 2a–d gives rise to 3a–d, accompanied by loss of [CpCo] fragment which could be captured by complex 1 to form a dinuclear species $(\text{CpCo})_2\text{S}_2\text{-C}_2\text{B}_{10}\text{H}_{10}$.^{25b,c} Note that in coordinative solvents such as THF, 2a–d can ideally convert to 3a–d with better carborene economy, which may be attributed to THF stabilization of intermediates such as V and VI', whereas in CH_2Cl_2 or toluene the conversion is less efficient as shown by the corresponding ratios of 2a–d:3a–d (SI, 1.1 and 4.1).

3. Redox Conversions of 2a–d and 3a–d. Formation of 4a–c and 5a–d. Despite electron unsaturation on cobalt, complexes 2a–d were found to be stable in air and moisture in both solution and solid state, with no detectable decomposition observed for 5 days in solution. However, when exposed to silica in air, visible transformation with color change from yellow to brown was observed, yielding oxidized products 4a–c and cobalt-free 5a–d (Scheme 3). The conversions could reach

Scheme 3. Synthesis of 4a–c and 5a–d by Treatment of 2a–d



good yields except 2d after overnight exposure. The crystal structure of 4a reveals that C(3)–S(2) bond has been cleaved and a novel norbornadienyl functional group is generated as shown in Figure 3a. The Co(1)–S(2) bond formation leads 4a as a diamagnetic 16e Co(III) species, thus allowing NMR analysis. In the ^1H NMR spectrum, a singlet at 8.12 ppm, which is assigned to H(3), is indicative of the new generated C(3)=C(4) bond. H(6) and H(7) appear at 6.76 and 7.16 ppm as typical vinyl proton signals. Two H(9) signals show characteristic doublets at 2.20 and 2.24 ppm with $J = 7.0$ Hz. By comparison of the ^1H coupled and ^1H decoupled ^{11}B spectra, B(3) that is attached to norbornadienyl was assigned at the lowest field (–0.8 ppm), and the others appear as overlapping signals at higher fields from –2.8 to –8.6 ppm. The ^{13}C signal of C(3) was observed at 161.0 ppm, and the two equal carborane carbons (C(1) and C(2)) show at 94.4 ppm. Notably, the generated 16e complexes 4a–c are stable to air and moisture.

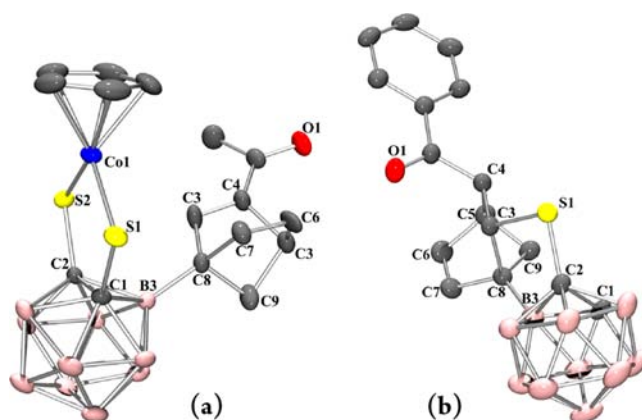


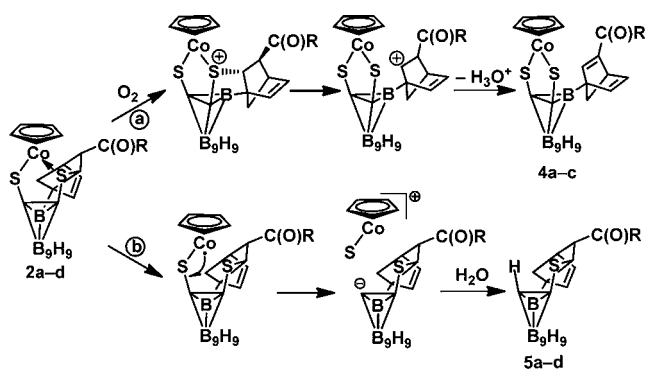
Figure 3. Crystal structures of 4a (a) and 5b (b). Select bond lengths [Å]: 4a, Co1–S1 2.1315, Co1–S2 2.1318, C1–C2 1.635(5), C3–C4 1.294(6), C6–C7 1.355(6), C8–B3 1.589(6); 5b, C1–C2 1.658(3), C2–S1 1.787(2), C3–S1 1.838(2), C3–C4 1.548(3), C6–C7 1.326(3), B3–C8 1.574(3).

5a–d were also isolated and characterized both in solution and solid state. Surprisingly, crystal structure of 5b (Figure 3b) shows that [CpCoS] fragment has been dissociated with a $\text{C}_{\text{cab}}\text{-H}$ (cab = carborane) bond recovery, but the original *endo* norbornyl moiety retains. Among the ^1H NMR signals of 5b, the newly formed $\text{C}_{\text{cab}}\text{-H}$ signal was observed at 3.77 ppm as a singlet. H(3) and H(4) were observed at 4.58 and 3.86 ppm, respectively, with a 5.0 Hz coupling, which is in agreement with *anti*-arrangement as revealed in solid state.³² H(6) appears at 6.03 ppm as a double of doublets ($J = 5.5, 2.5$ Hz). Because of the binding to norbornyl, the ^{11}B resonance of B(3) is located at 1.1 ppm, which is the lowest one among all the boron signals. In the ^{13}C NMR spectrum, C(3) is shifted to the lower field at 69.7 ppm compared to other alkyl signals (e.g., C(4) at 53.4 ppm) as it is attached to the carboranyl thiolate unit. Two carborane skeletal carbons show signals at 73.6 and 84.0 ppm. It follows the consistent structures both in solution and solid state.

The conversions of 2a–d to 4a–c and 5a–d involve both alkyl and carboranyl C–S cleavage. Similar metal-induced alkyl C–S cleavage leading to vinyl derivatives has been extensively reported,³³ whereas carboranyl C–S cleavage is fairly rare; for example, the carboranyl cyclothioether cleavage was induced only by electrochemical methods.³⁴ In this study the alkyl C–S cleavage to 4a–c is more competitive (>67%), and carboranyl C–S cleavage to 5a–d plays a minor role (<21%).

Possible Mechanisms for the Formation of 4a–c and 5a–d. The simple but specific combination of air, silica and moisture has led to efficient conversions of 2a–d to 4a–c and 5a–d bearing a boron-norbornadienyl or a boron-norbornyl group at carborane. Obviously, the valence alteration from Co(II) to Co(III) indicates an oxidation process involved. Possible formation on 4a–c is shown in Scheme 4a. In the presence of air, Co(II) is oxidized to Co(III) to form covalent Co–S bond and sulfonium intermediate, which subsequently leads to 4a–c via C(3)–S bond cleavage and loss of proton. Note that no conversion was observed in the absence of any of silica, air or moisture. Here silica might act as both a catalyst and a carrier of O_2 and moisture. In contrast, the formation of 5a–d proceeds via a reductive-type pathway (Scheme 4b), where Co(II) acts as the reductant. Initiated by electron transfer,³⁵ the carboranyl C–S cleavage gives rise to a [5d –

Scheme 4. Possible Pathways of 2a–d Conversions through Alkyl C–S (a) and Carboranyl C–S (b) Cleavage

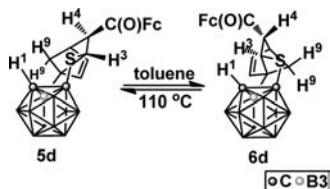


H^- , anion and the resulting $[\text{CpCoS}]$ fragment is likely absorbed on silica. Comparative experiment by treatment of 2a–d with NaBH_4 (in THF) led to similar yields of 5a–d but no formation of 4a–d, further supporting the proposed reductive C–S cleavage (SI, 5.3).

The 17e complexes 3a–d are more stable to air and moisture than 2a–d; however, under the same conditions they can also finally convert to 5a–d with similar yields. In monitoring the conversion of 3d to 5d, an intermediate with *syn*-C(O)Fc group was observed by ^1H NMR (SI, 5.4), which gradually isomerizes to 5d, indicating that reorientation of $-\text{C}(\text{O})\text{Fc}$ from *syn* back to *anti* is not a quick process.

Retro-Diels–Alder Reaction of 5d. In Diels–Alder studies, one can often encounter isomers with *endo/exo* configurations according to different cycloaddition type. It is commonly accepted that *endo* is kinetically controlled while *exo* is thermodynamically controlled.³⁶ Therefore it is expected that in this study the *endo* boron-norbornyl products are possible to transform under thermal conditions. Refluxing in toluene (110 °C) for 10 h, 5d led to a new isomer 6d in 45% yield with 5d remaining in 49%. In reverse, treatment of the isolated 6d led to a 40% conversion to 5d, indicating an equilibrium between the two isomers (Scheme 5). EI-MS analysis of each gave

Scheme 5. Thermal Interconversion between 5d and 6d



molecular ion peak at m/z 478.2. The crystal structures of 5d and 6d (Figure 4) reveal the *endo* norbornyl moiety in both cases, rather than the common *endo/exo* modes.³⁷ The difference between 5d and 6d is the skeleton configuration of norbornyl group (i.e., R^3, S^4, S^5, R^8 -5d and S^3, R^4, R^5, S^8 -6d). This is also reflected in individual NMR data. Despite the same 5.0 Hz coupling of $J_{\text{H}(3)-\text{H}(4)}$ in both 5d and 6d, the H(3) signal in 5d (4.57 ppm) is shifted to 4.06 ppm in 6d. H(1) signal of 5d appears at 3.76 ppm but is shifted to 3.92 ppm in 6d. The chemical shifts of H(9) protons are changed from 1.98/1.70 ppm in 5d to 2.27/1.88 ppm in 6d. All these might indicate the steric neighborhood effect between H(1)/H(9) in 5d and H(1)/H(3) in 6d. The alternation of norbornyl group also led to obvious ^{11}B NMR signal shifts that boron signals of 6d have

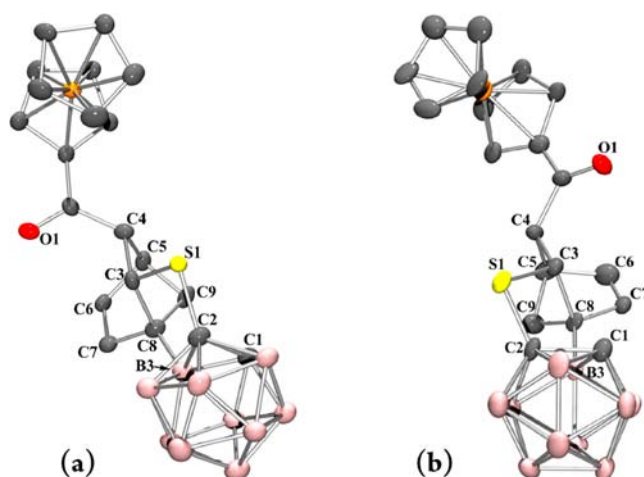


Figure 4. Crystal structures of 5d (a) and 6d (b). Select bond lengths [Å]: 5d, C1–C2 1.632(5), C3–C4 1.557(4), C6–C7 1.380(4), B3–C8 1.588(5); 6d, C1–C2 1.651(5), C3–C4 1.554(5), C6–C7 1.325(6), B3–C8 1.572(5).

moved to low field by 0.5–2.5 ppm relative to those in 5d. A significant ^{13}C signal shift was observed on C(1) from 5d (73.6 ppm) to 6d (63.2 ppm).

The interconversion between 5d and 6d can be considered as retro-Diels–Alder/Diels–Alder processes.³⁸ To get a better understanding, the calculated energy profile (under m06/6-31g(d,p)/lanl2dz level) is provided in Figure 5. Recognizing

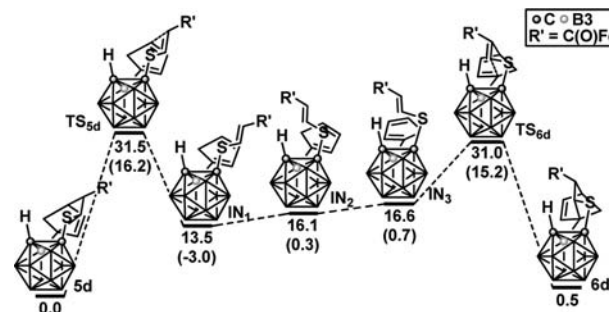
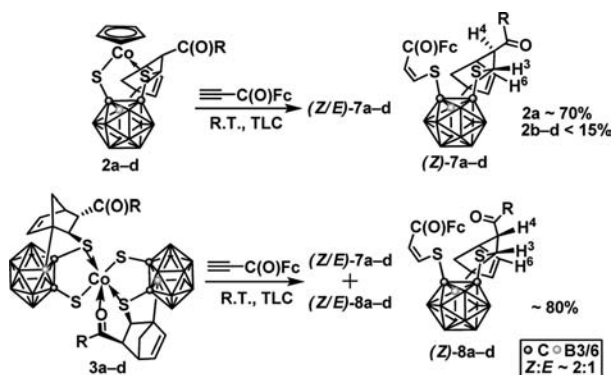


Figure 5. Relative free energy profile (kcal/mol, at 298 K, values given in the bracket, at 383 K) calculated for conversion of 5d to 6d.

from the relative free energy of each intermediate or transition state, the conversion only occurs after overcoming the high energy barrier for retro-Diels–Alder process (TS_{5d} , 31.5 kcal/mol vs TS_{6d} , 31.0 kcal/mol, 298 K), in agreement with observed temperature dependence (no reaction would occur at room temperature). In this case, conversion from IN_1 to IN_3 proceeds without high energetic obstacles ($\Delta G = 3.1$ kcal/mol). Because of the approximately equal energy change to either side, a similar distribution between 5d and 6d is expected, as was experimentally observed. Optimized structures also supply clues for the origin of stereoselectivity. Following the steric requirement, the $[4 + 2]$ cycloaddition will not respond if the orientation of dienophile and diene disagrees; thus, B–Cp in IN_1 would not match vinyl group in IN_3 unless a 147° rotation (see IN_1 and IN_3 coordinates, SI, 6.5) occurs where specific *endo* configuration is produced. Since limited by inner strain, the *exo* isomer is excluded. For this reason, the interconversion of boron-norbornyl moiety acts as a special example in the Diels–Alder/retro-Diels–Alder chemistry.

4. Alkyne Insertion into 2a–d and 3a–d. Reactions of 2a–d and 3a–d toward Alkynes. Not only is the reactivity of 17e complexes **2a–d** and **3a–d** reflected in the redox conversions owing to the unsaturated metal center as discussed above, but also the reactive Co–S bond as in **1** predicts reactivity toward alkynes. The ferrocenyl-conjugated alkyne $\text{HC}\equiv\text{CC}(\text{O})\text{Fc}$ was chosen for this study on the basis of ease of isolation (color indicator) and the useful redox properties of ferrocenyl derivatives in biological systems.³⁹ The reactions of **2a–d** and $\text{HC}\equiv\text{CC}(\text{O})\text{Fc}$ at ambient temperature led to new cobalt-free compounds (*Z/E*)-**7a–d**, and **3a–d** led to additional compounds (*Z/E*)-**8a–d**, as illustrated in Scheme 6. The

Scheme 6. Reactions of **2a–d** and **3a–d** with $\text{HC}\equiv\text{CC}(\text{O})\text{Fc}$ in Either THF or CH_2Cl_2



molecular structures of (*Z*)-**7d**, (*E*)-**7d** and (*Z*)-**8d** were characterized by X-ray diffraction, and two are shown in Figure 6 (see SI, 2.2, for (*E*)-**7d**). Apparently, (*Z/E*)-**7d** retain the *endo* norbornyl moiety from **2d** accordingly, and the other carbon at carborane is consequently substituted by *Z/E* vinyl sulfido unit. The ^1H NMR data also confirm the *endo* configuration with $J_{\text{H}(3)-\text{H}(4)} = 5.0$ Hz in both cases, but $J_{\text{H}(10)-\text{H}(11)}$ is characteristic for (*Z/E*)-**7d** with values of 10.0 and 15.0 Hz, respectively. Other significantly different ^1H signals of the two isomers were observed at 7.37, 6.76 ppm for (*Z*)- $\text{CH}=\text{CHC}(\text{O})\text{Fc}$ and 2.85, 1.70 ppm for H(9) in (*Z*)-**7d** in contrast to 7.71, 6.82 ppm for (*E*)- $\text{CH}=\text{CHC}(\text{O})\text{Fc}$ and 2.68, 1.65 ppm for H(9) in (*E*)-**7d**. A major characteristic of (*Z/E*)-**8d** that distinguishes it from (*Z/E*)-**7d** is the *syn*-arrangement of $-\text{C}(\text{O})\text{Fc}$ group that inherits from **3d** (Figure 6), as supported by a larger coupling constant $J_{\text{H}(3)-\text{H}(4)} = 9.0$ Hz. The different orientation of $-\text{C}(\text{O})\text{Fc}$ group has led to H(6) signal in (*Z*)-**8d** (6.38 ppm) high-field shift by 0.35 ppm from that in (*Z*)-**7d** (6.03 ppm) and H(4) signal of (*Z*)-**8d** (3.10 ppm) low-field shift by 0.47 ppm relative to (*Z*)-**7d** (3.57 ppm).

The insertion of $\text{HC}\equiv\text{CC}(\text{O})\text{Fc}$ toward **2a** occurs in 70% yield at ambient temperature, whereas **2b–d** proceed in less than 15% with both reactants remaining under the identical condition. The distribution of isomers *Z:E* is $\sim 2:1$ for all R groups investigated. Similar reactions toward **3a–d** (Scheme 6) are more efficient with yields of around 80%. The distribution of the four isomers show (*Z*)-**7b** \approx (*Z*)-**8b** and (*E*)-**7b** \approx (*E*)-**8b**, as expected. Methyl derivatives from **3a** are against this trend with (*Z/E*)-**7a** being predominant, which might be caused by easier reorientation of the small acetyl group. Generally, the presence of additional vinyl sulfido group on carborane efficiently blocks reorientation of $-\text{C}(\text{O})\text{R}$ within

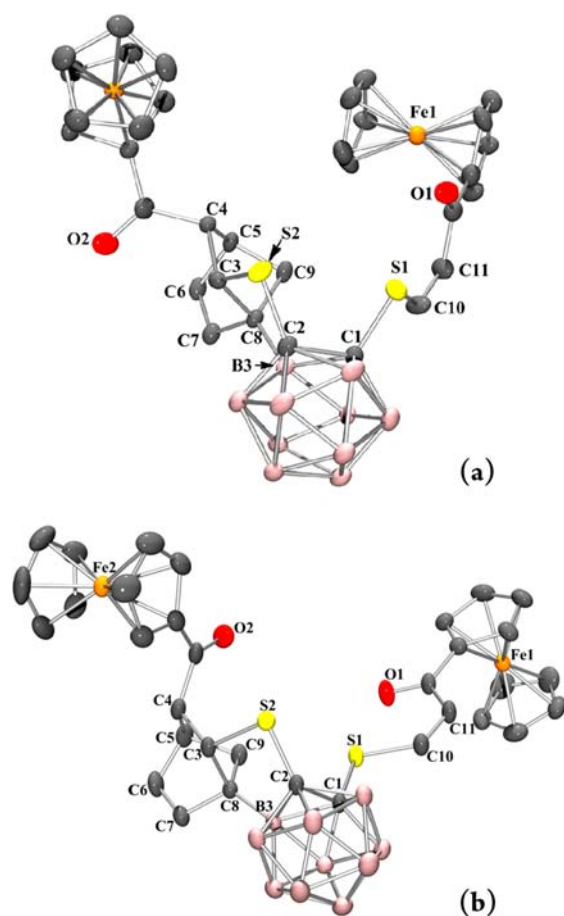
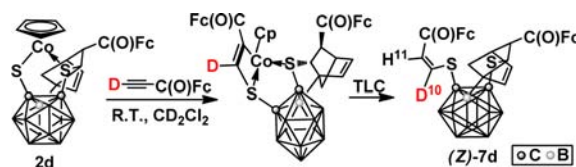


Figure 6. Crystal structures of (*Z*)-**7d** (a) and (*Z*)-**8d** (b). Select bond lengths [\AA]: **7d**, C1–C2 1.767(5), C3–C4 1.543(5), C6–C7 1.328(5), C10–C11 1.333(6), B3–C8 1.564(5); **8d**, C1–C2 1.801(5), C3–C4 1.553(5), C6–C7 1.311(6), C10–C11 1.336(5), B3–C8 1.572(5).

norbornyl unit; thus, (*Z/E*)-**8a–d** can be isolated. This differs from the reduction of **3a–d** to form **5a–d** where $-\text{C}(\text{O})\text{R}$ group could turn from *syn* to *anti* conformations (SI, 5.4). In this study differing orientations of $-\text{C}(\text{O})\text{R}$ group contribute variety of structural isomers containing norbornyl unit at carborane.

Possible formation of (*Z/E*)-**7a–d** was investigated by reaction of **2d** with excess $\text{DC}\equiv\text{CC}(\text{O})\text{Fc}$ in CD_2Cl_2 (Scheme 7). Deuterated (*Z*)-**7d** was isolated by TLC and its ^1H NMR

Scheme 7. Proposed Formation of (*Z*)-**7d** by Deuterium Labeling Experiment

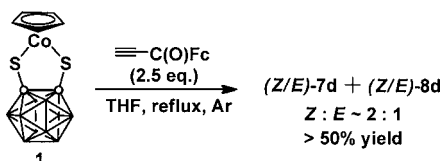


spectrum shows a similar deuterium degree for H(10) as in starting $\text{DC}\equiv\text{CC}(\text{O})\text{Fc}$, but H(11) signal remains unaffected (SI, Figure S5.5.2), indicating that this hydrogen does not originate from excess deuterated alkyne. Thus alkyne insertion into Co–S bond, followed by demetalation through a hydrolytic process on silica was proposed (Scheme 7). As

such, the steric factor of Cp ligand from **2a–d** should be responsible for the lower conversions relative to **3a–d**.

One-Pot Synthesis of B–H Functionalized Carborane Derivatives. On the basis of the favored formation of **3a–d** from complex **1** in THF and efficient alkyne insertion toward **3a–d**, the strategy of using complex **1** with excess alkyne was anticipated to straightforwardly prepare boron-norbornyl products. Indeed, the reaction of complex **1** and $\text{HC}\equiv\text{CC}(\text{O})\text{Fc}$ in refluxed THF led to (Z/E)-**7d** and (Z/E)-**8d** (Scheme 8) in a yield of over 50% with no observed **2d** and **3d**,

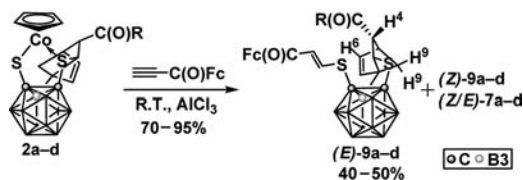
Scheme 8. One-Pot Synthesis of (Z/E)-7d and (Z/E)-8d



and the distribution of four isomers is close to that obtained from **3d**. It is interesting that from the neat result of the one-pot synthesis, the ancillary ligand Cp, generally less reactive, is efficiently involved in in situ construction of organic boron-norbornyl carborane derivatives without need of tedious isolation of **17e** intermediates. No doubt that the electron-deficient terminal alkynes are suitable for this strategy as such alkynes fit both regio- and stereoselectivity in alkyne insertion into Co–S bond as well as the requirement for Diels–Alder addition.

Lewis Acid (e.g., AlCl_3) Improves Reactivity and Selectivity to Form (E)-9a–d. Electron-deficient alkynes, such as $\text{MeO}_2\text{CC}\equiv\text{CCO}_2\text{Me}$, exhibited excellent reactivity toward Co–S bond to alkyne insertion adducts.²⁵ On considering that Lewis acids such as AlCl_3 can further increase electron deficiency of carbonyl-substituted alkynes through oxygen-coordination,⁴⁰ AlCl_3 was anticipated to improve the low reactivity of $\text{HC}\equiv\text{CC}(\text{O})\text{Fc}$ and **2a–d** shown in Scheme 6. As predicted, addition of AlCl_3 at room temperature resulted in conversions of 70–95% in contrast to less than 15% in the absence of AlCl_3 . More surprisingly, additional products (E)-**9a–d** were generated as major products accounting for 40–50% yields (Scheme 9). The molecular structure of this series is

Scheme 9. AlCl_3 -Mediated Reactions of **2a–d and $\text{HC}\equiv\text{CC}(\text{O})\text{Fc}$ Leading to (E)-9a–d as Major Products**



proven by a Z-isomer, for example, (Z)-**9b** in Figure 8a with a ferrocenyl-conjugated vinyl sulfido unit attached to carborane, which is generated from alkyne insertion. In comparison with **2b**, the norbornyl moiety in (Z)-**9b** exhibits an alternative *endo* configuration, which is derived from a retro-Diels–Alder process as occurred from **5d** to **6d**. This change has resulted in significant differences of ^1H data for H(9) protons, for example, 2.43, 1.97 ppm in (Z)-**9b** vs 2.93, 1.71 ppm in (Z)-**7b**.

The carbonyl oxygen-coordination to AlCl_3 not only leads to further alkyne activation thus improving yields, but also

considerably increases *E*-selectivity attributed to restricted isomerization from original *E*- to *Z*-configuration. Here AlCl_3 also plays an additional role in facilitating *endo/endo* conversion of the norbornyl moiety as the alkyl derivatives of AlCl_3 often act as catalysts for Diels–Alder/retro-Diels–Alder reactions.⁴¹ A comparison of the ^1H NMR spectra of the products from reaction of **2a** and $\text{HC}\equiv\text{CC}(\text{O})\text{Fc}$ (Figure 7) shows that upon addition of AlCl_3 , the ratio of *E/Z* is increased from 33:67 to 65:35, and (E)-**9a** accounts for 51%.

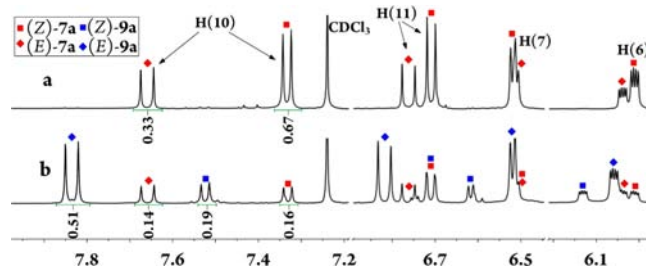
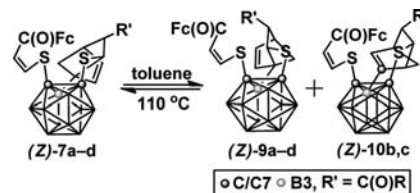


Figure 7. Selected ^1H NMR spectra for comparison of the products from **2a and $\text{HC}\equiv\text{CC}(\text{O})\text{Fc}$: (a) AlCl_3 -free reaction led to (Z/E)-**7a**; (b) AlCl_3 -mediated reaction led to (Z/E)-**7a** and (Z/E)-**9a**.**

Retro-Diels–Alder Study on (Z/E)-7a–d. The retro-Diels–Alder reactions of (Z)-**7a–d** were studied in refluxed toluene. As a result, (Z)-**9a–d** (30–50%) and unexpected products (Z)-**10b,c** (25 and 33%) were isolated together with unreacted (Z)-**7a–d** (30–45%) (Scheme 10). The ^1H NMR monitoring

Scheme 10. Synthesis of (Z)-9a–d and (Z)-10b,c



confirmed that no *E*-isomers were in this reaction. The crystal structure of (Z)-**10b** (Figure 8b) reveals a different boron-norbornyl unit where B(3) is bound to C(7), rather than C(8) as in the other products, indicative of H-shift occurrence during the retro-Diels–Alder process. Correspondingly, boron-norbornyl moiety in (Z)-**10b** has significantly different NMR data. For example, H(6) appears at 7.17 ppm, low-field shifted in comparison to 5.96 ppm in (Z)-**7b** or 6.08 ppm in (Z)-**9b** because of the electron-withdrawing effect of carborane cage. The new H(8) proton is located at 4.12 ppm. Another distinct feature was observed in the separation of the two H(9) signals for 0.17 ppm in (Z)-**10b**, much smaller than those in (Z)-**9b** (0.46 ppm) and (Z)-**7b** (1.22 ppm). The ^{13}C NMR spectrum shows a weak and broad peak at 133.8 ppm assigned to C(7)–B(3).

The formation of (Z)-**10b,c** is a selection of cycloaddition between diene and dienophile in the retro-Diels–Alder process. This might be explained that synchronous vinyl reorientation and B–Cp rotation give (Z)-**9a–d**, but if [1,2]-H migration within Cp occurs during B–Cp rotation, (Z)-**10b,c** would be formed. Such a phenomenon has not been described in any retro-Diels–Alder reaction, but here the [1,2]-H migration has led to a new type of B–Cp precursors for the following Diels–Alder process, thus contributing diversity of the boron-

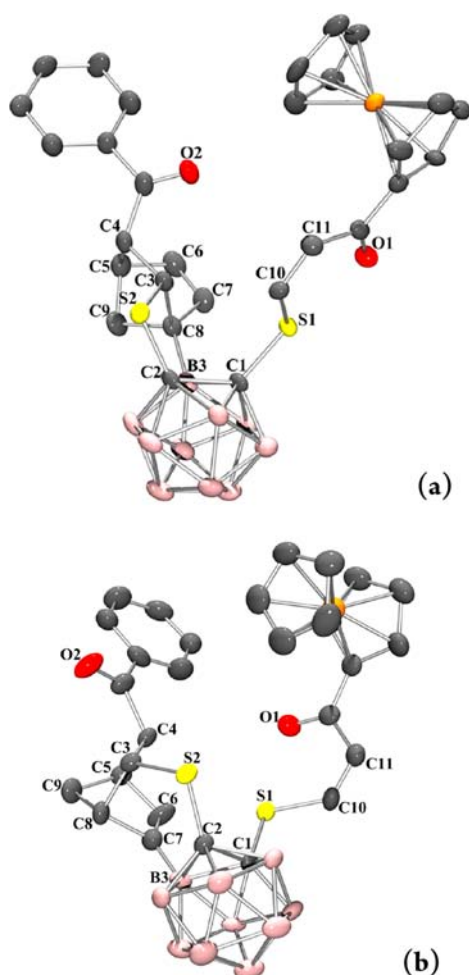


Figure 8. Crystal structures of (Z)-9b (a) and (Z)-10b (b). Select bond lengths [Å]: (Z)-9b, C1–C2 1.691(4), C3–C4 1.545(5), C6–C7 1.338(6), C10–C11 1.348(5), B3–C8 1.606(5); (Z)-10b, C1–C2 1.784(6), C3–C4 1.579(6), C6–C7 1.332(7), C7–C8 1.553(6), C10–C11 1.337(7), B3–C7 1.436(7).

functionalized carborane family. Moreover, the conversions of (*E*)-7a–d were investigated as well, and additional transformation from *E* to *Z* configuration was observed. If a longer time was applied (i.e., 30 h), the same product distribution was eventually reached as starting from (*Z*)-7a–d.

CONCLUSIONS

Two types of 17e cobalt(II) complexes containing B(3)/B(6)-norbornyl carborane have been synthesized from CpCoS₂C₂B₁₀H₁₀ (**1**) and electron-deficient alkynes HC≡CC(O)R at ambient temperature. Their formation includes metal-induced selective B–H activation, B–Cp formation and Cp-involved Diels–Alder addition, as supported by DFT calculations. These isolatable 17e intermediates exhibit interesting redox reactions under simple conditions that has led to both alkyl C–S cleavage and carboranyl C–S cleavage to yield stable 16e Co(III) complexes bearing a boron-norbornadienyl unit and organic carborane derivatives bearing a boron-norbornyl group, respectively. The reactive Co–S bonds provide further reactivity toward alkynes that has delivered two series of cobalt-free carborane derivatives containing a B(3)-norbornyl moiety. In particular, the one-pot reactions of complex **1** and alkynes HC≡CC(O)R under

mild conditions allow for straightforward norbornyl functionalization at B(3)/B(6) sites of carborane in good yields. Two strategies using thermal promotion or Lewis acid mediation have provided specific retro-Diels–Alder products with differing boron-norbornyl groups and good selectivity. In this study cobalt-mediated selective B–H activation and further functionalization has provided a facile and efficient route to a new family of functionalized carborane derivatives containing either norbornadienyl or norbornyl group.

ASSOCIATED CONTENT

Supporting Information

Experimental section and crystallographic data (CIF) are available free of charge via the Internet at <http://pubs.acs.org>.

AUTHOR INFORMATION

Corresponding Author

hyan1965@nju.edu.cn

Notes

The authors declare no competing financial interest.

ACKNOWLEDGMENTS

We thank Prof. Zhenyang Lin and Prof. You Song for their helpful suggestions. This work was supported by the National Basic Research Program of China (2010CB923303 and 2013CB922101), the National Science Foundation of China (20925104, 21271102 and 21021062) and high performance computational center of Nanjing University. Dedicated to Professor Dr. Vladimir Bregadze on the occasion of his 75th birthday.

REFERENCES

- (1) (a) Hosmane, N. S. *Boron Science: New Technologies and Applications*; CRC Press: Boca Raton, FL, 2011. (b) Grimes, R. N. *Coord. Chem. Rev.* **2000**, *200*, 773. (c) Wedge, T. J.; Hawthorne, M. F. *Coord. Chem. Rev.* **2003**, *240*, 111. (d) Hawthorne, M. F.; Zink, J. I.; Skelton, J. M.; Bayer, M. J.; Liu, C.; Livshits, E.; Baer, R.; Neuhauser, D. *Science* **2004**, *303*, 1849. (e) Jude, H.; Disteldorf, H.; Fischer, S.; Wedge, T.; Hawkridge, A. M.; Arif, A. M.; Hawthorne, M. F.; Muddiman, D. C.; Stang, P. J. *J. Am. Chem. Soc.* **2005**, *127*, 12131. (f) Farha, O. K.; Spokoyny, A. M.; Mulfort, K. L.; Hawthorne, M. F.; Mirkin, C. A.; Hupp, J. T. *J. Am. Chem. Soc.* **2007**, *129*, 12680. (g) Dash, B. P.; Satapathy, R.; Gaillard, E. R.; Maguire, J. A.; Hosmane, N. S. *J. Am. Chem. Soc.* **2010**, *132*, 6578. (h) Saxena, A. K.; Hosmane, N. S. *Chem. Rev.* **1993**, *93*, 1081. (i) Saxena, A. K.; Maguire, J. A.; Hosmane, N. S. *Chem. Rev.* **1997**, *97*, 2421. (j) Shi, C.; Sun, H. B.; Jiang, Q. B.; Zhao, Q.; Wang, J. X.; Huang, W.; Yan, H. *Chem. Commun.* **2013**, *49*, 4746.
- (2) (a) Xie, Z. W. *Coord. Chem. Rev.* **2006**, *250*, 259. (b) Vives, G.; Tour, J. M. *Acc. Chem. Res.* **2009**, *42*, 473. (c) Pepiol, A.; Teixidor, F.; Saralidze, K.; van der Marel, C.; Willems, P.; Voss, L.; Knetsch, M. L. W.; Vinas, C.; Koole, L. H. *Biomaterials* **2011**, *32*, 6389. (d) Pieters, G.; Gaucher, A.; Prim, D.; Besson, T.; Planas, J. G.; Teixidor, F.; Vinas, C.; Light, M. E.; Hursthouse, M. B. *Chem. Commun.* **2011**, *47*, 7725. (e) Puga, A. V.; Teixidor, F.; Sillanpaa, R.; Kivekas, R.; Vinas, C. *Chem. Commun.* **2011**, *47*, 2252. (f) Teixidor, F.; Nunez, R.; Flores, M. A.; Demonceau, A.; Vinas, C. *J. Organomet. Chem.* **2000**, *614*, 48. (g) Wee, K. R.; Cho, Y. J.; Jeong, S.; Kwon, S.; Lee, J. D.; Suh, I. H.; Kang, S. O. *J. Am. Chem. Soc.* **2012**, *134*, 17982. (h) Wee, K. R.; Han, W. S.; Cho, D. W.; Kwon, S.; Pac, C.; Kang, S. O. *Angew. Chem., Int. Ed.* **2012**, *51*, 2677.
- (3) (a) Bregadze, V. I.; Sivaev, I. B.; Glazun, S. A. *Anti-Cancer Agents Med. Chem.* **2006**, *6*, 75. (b) Hawthorne, M. F. *Angew. Chem., Int. Ed.* **1993**, *32*, 950. (c) Hawthorne, M. F.; Maderna, A. *Chem. Rev.* **1999**, *99*, 3421. (d) Sivaev, I. B.; Bregadze, V. V. *Eur. J. Inorg. Chem.* **2009**,

- 11, 1433. (e) Valliant, J. F.; Guenther, K. J.; King, A. S.; Morel, P.; Schaffer, P.; Sogbein, O. O.; Stephenson, K. A. *Coord. Chem. Rev.* **2002**, *232*, 173. (f) Scholz, M.; Hey-Hawkins, E. *Chem. Rev.* **2011**, *111*, 7035. (g) Barry, N. P. E.; Sadler, P. J. *Chem. Soc. Rev.* **2012**, *41*, 3264. (h) Yinghuai, Z.; Peng, A. T.; Carpenter, K.; Maguire, J. A.; Hosmane, N. S.; Takagaki, M. *J. Am. Chem. Soc.* **2005**, *127*, 9875. (i) Cigler, P.; Kozisek, M.; Rezacova, P.; Brynda, J.; Otwinowski, Z.; Pokorna, J.; Plesek, J.; Gruner, B.; Doleckova-Maresova, L.; Masa, M.; Sedlacek, J.; Bodem, J.; Krausslich, H. G.; Kral, V.; Konvalinka, J. *Proc. Natl. Acad. Sci. U. S. A.* **2005**, *102*, 15394. (j) Wu, C. H.; Wu, D. H.; Liu, X.; Guoyiqibayi, G.; Guo, D. D.; Lv, G.; Wang, X. M.; Yan, H.; Jiang, H.; Lu, Z. H. *Inorg. Chem.* **2009**, *48*, 2352. (k) Wu, C. H.; Shi, L. X.; Li, Q. N.; Jiang, H.; Selke, M.; Yan, H.; Wang, X. M. *Nanomedicine* **2012**, *8*, 860. (l) Dou, H.; Zhong, W.; Hou, Y. Y.; Yan, H. *Bioorg. Med. Chem.* **2012**, *20*, 4693. (m) Li, S. H.; Wang, Z. J.; Wei, Y. F.; Wu, C. Y.; Gao, S. P.; Jiang, H.; Zhao, X. Q.; Yan, H.; Wang, X. M. *Biomaterials* **2013**, *34*, 902.
- (4) Bregadze, V. I. *Chem. Rev.* **1992**, *92*, 209.
- (5) Grimes, R. N. *Carboranes*, 2nd ed.; Academic Press: New York, 2011.
- (6) (a) Zakharkin, L. I.; Olshevskaya, V. A.; Vorontsov, E. V.; Petrovsky, P. V. *Russ. Chem. Bull.* **1996**, *45*, 2614. (b) Herzog, A.; Maderna, A.; Harakas, G. N.; Knobler, C. B.; Hawthorne, M. F. *Chem.—Eur. J.* **1999**, *5*, 1212. (c) Dash, B. P.; Satapathy, R.; Maguire, J. A.; Hosmane, N. S. *Org. Lett.* **2008**, *10*, 2247.
- (7) (a) Zakharkin, L. I.; Kalinin, V. N. *Izv. Akad. Nauk SSSR, Ser. Khim.* **1966**, *169*, 590. (b) Zheng, Z. P.; Jiang, W.; Zinn, A. A.; Knobler, C. B.; Hawthorne, M. F. *Inorg. Chem.* **1995**, *34*, 2095.
- (8) (a) Plesek, J.; Janousek, Z.; Hermanek, S. *Collect. Czech. Chem. Commun.* **1980**, *45*, 1775. (b) Plesek, J.; Janousek, Z.; Hermanek, S. *Inorg. Synth.* **1983**, *22*, 241. (c) Spokoiny, A. M.; Machan, C. W.; Clingerman, D. J.; Rosen, M. S.; Wiester, M. J.; Kennedy, R. D.; Stern, C. L.; Sarjeant, A. A.; Mirkin, C. A. *Nat. Chem.* **2011**, *3*, 590.
- (9) (a) Potenza, J. A.; Lipscomb, W. N. *Inorg. Chem.* **1966**, *5*, 1471. (b) Potenza, J. A.; Lipscomb, W. N.; Vickers, G. D.; Schroede, H. J. *Am. Chem. Soc.* **1966**, *88*, 628.
- (10) (a) Barbera, G.; Vaca, A.; Teixidor, F.; Sillanpaa, R.; Kivekas, R.; Vinas, C. *Inorg. Chem.* **2008**, *47*, 7309. (b) Qiu, Z.; Xie, Z. *J. Am. Chem. Soc.* **2010**, *132*, 16085.
- (11) (a) Hoel, E. L.; Hawthorne, M. F. *J. Am. Chem. Soc.* **1973**, *95*, 2712. (b) Hoel, E. L.; Hawthorne, M. F. *J. Am. Chem. Soc.* **1974**, *96*, 6770. (c) Hoel, E. L.; Hawthorne, M. F. *J. Am. Chem. Soc.* **1975**, *97*, 6388.
- (12) (a) Prokhorov, A. M.; Slepukhin, P. A.; Rusinov, V. L.; Kalinin, V. N.; Kozhevnikov, D. N. *Chem. Commun.* **2011**, *47*, 7713. (b) Fey, N.; Haddow, M. F.; Mistry, R.; Norman, N. C.; Orpen, A. G.; Reynolds, T. J.; Pringle, P. G. *Organometallics* **2012**, *31*, 2907.
- (13) (a) Hewes, J. D.; Kreimendahl, C. W.; Marder, T. B.; Hawthorne, M. F. *J. Am. Chem. Soc.* **1984**, *106*, 5757. (b) Du, S. W.; Ellis, D. D.; Jelliss, P. A.; Kautz, J. A.; Malget, J. M.; Stone, F. G. A. *Organometallics* **2000**, *19*, 1983. (c) Du, S. W.; Kautz, J. A.; McGrath, T. D.; Stone, F. G. A. *Chem. Commun.* **2002**, 1004. (d) Meneghelli, B. J.; Rudolph, R. W. *J. Am. Chem. Soc.* **1978**, *100*, 4626.
- (14) (a) Mirabelli, M. G. L.; Sneddon, L. G. *J. Am. Chem. Soc.* **1988**, *110*, 449. (b) Wilczynski, R.; Sneddon, L. Y. *Inorg. Chem.* **1982**, *21*, 506. (c) Corcoran, E. W. Jr.; Sneddon, L. G. In *Advances in Boron and the Boranes*; Liebman, J. F., Greenberg, A., Williams, R. E., Eds.; VCR: New York, 1988; p 71.
- (15) (a) Herberhold, M.; Yan, H.; Milius, W.; Wrackmeyer, B. *Angew. Chem., Int. Ed.* **1999**, *38*, 3689. (b) Herberhold, M.; Yan, H.; Milius, W.; Wrackmeyer, B. *Chem.—Eur. J.* **2002**, *8*, 388. (c) Wrackmeyer, B.; Yan, H.; Milius, W.; Herberhold, M. *Russ. Chem. Bull.* **2001**, *50*, 1518. (d) Herberhold, M.; Yan, H.; Milius, W.; Wrackmeyer, B. *Chem.—Eur. J.* **2000**, *6*, 3026. (e) Bai, W.; Liu, G.; Guoyiqibayi, G.; Yan, H. *Organometallics* **2011**, *30*, 5188. (f) Herberhold, M.; Yan, H.; Milius, W.; Wrackmeyer, B. *J. Organomet. Chem.* **2000**, *604*, 170. (g) Li, Y.; Jiang, Q.; Zhang, X.; Li, Y.; Yan, H.; Bregadze, V. I. *Inorg. Chem.* **2010**, *49*, 3911. (h) Xu, B. H.; Tao, J. C.; Li, Y. Z.; Li, S. H.; Yan, H. *Organometallics* **2008**, *27*, 334. (i) Liu, G.; Hu, J.; Wen, J.; Dai, H.; Li, Y.; Yan, H. *Inorg. Chem.* **2011**, *50*, 4187.
- (16) Zhang, R.; Zhu, L.; Liu, G.; Dai, H.; Lu, Z.; Zhao, J.; Yan, H. *J. Am. Chem. Soc.* **2012**, *134*, 10341.
- (17) Li, Y.; Jiang, Q.; Li, Y.; Yan, H.; Bregadze, V. I. *Inorg. Chem.* **2010**, *49*, 4.
- (18) Davis, J. C.; Vanauken, T. V. *J. Am. Chem. Soc.* **1965**, *87*, 3900.
- (19) (a) Xu, B. H.; Peng, X. Q.; Xu, Z. W.; Li, Y. Z.; Yan, H. *Inorg. Chem.* **2008**, *47*, 7928. (b) McNamara, W. R.; Han, Z.; Alperin, P. J.; Brennessel, W. W.; Holland, P. L.; Eisenberg, R. *J. Am. Chem. Soc.* **2011**, *133*, 15368.
- (20) (a) Xi, Z. F.; Sato, K.; Gao, Y.; Lu, J. M.; Takahashi, T. *J. Am. Chem. Soc.* **2003**, *125*, 9568. (b) Sun, Y.; Chan, H. S.; Zhao, H. T.; Lin, Z. Y.; Xie, Z. W. *Angew. Chem., Int. Ed.* **2006**, *45*, 5533. (c) Takahashi, T.; Kuzuba, Y.; Kong, F.; Nakajima, K.; Xi, Z. F. *J. Am. Chem. Soc.* **2005**, *127*, 17188. (d) Takahashi, T.; Song, Z. Y.; Sato, K.; Kuzuba, Y.; Nakajima, K.; Kanno, K. I. *J. Am. Chem. Soc.* **2007**, *129*, 11678. (e) Takahashi, T.; Song, Z. Y.; Hsieh, Y. F.; Nakajima, K.; Kanno, K. *J. Am. Chem. Soc.* **2008**, *130*, 15236. (f) Ren, S. Y.; Igarashi, E.; Nakajima, K.; Kanno, K.; Takahashi, T. *J. Am. Chem. Soc.* **2009**, *131*, 7492.
- (21) (a) Fruhauf, H. W. *Chem. Rev.* **1997**, *97*, 523. (b) Boag, N. M.; Rao, K. M. *Chem. Commun.* **2009**, *12*, 1499.
- (22) Zhao, Y.; Truhlar, D. G. *Theor. Chem. Acc.* **2008**, *120*, 215.
- (23) (a) Hay, P. J.; Wadt, W. R. *J. Chem. Phys.* **1985**, *82*, 270. (b) Wadt, W. R.; Hay, P. J. *J. Chem. Phys.* **1985**, *82*, 284. (c) Hay, P. J.; Wadt, W. R. *J. Chem. Phys.* **1985**, *82*, 299. (d) Check, C. E.; Faust, T. O.; Bailey, J. M.; Wright, B. J.; Gilbert, T. M.; Sunderlin, L. S. *J. Phys. Chem. A* **2001**, *105*, 8111. (e) Chiodo, S.; Russo, N.; Sicilia, E. *J. Chem. Phys.* **2006**, *125*, 104107.
- (24) (a) Takatani, T.; Sears, J. S.; Sherrill, C. D. *J. Phys. Chem. A* **2010**, *114*, 11714. (b) Supporting Information for Zhong, W.; Yang, Q.; Shang, Y.; Liu, G.; Zhao, H.; Li, Y.; Yan, H. *Organometallics* **2012**, *31*, 6658.
- (25) (a) Xu, B. H.; Peng, X. Q.; Li, Y. Z.; Yan, H. *Chem.—Eur. J.* **2008**, *14*, 9347. (b) Kim, D. H.; Ko, J. J.; Park, K.; Cho, S. G.; Kang, S. O. *Organometallics* **1999**, *18*, 2738. (c) Won, J. H.; Kim, D. H.; Kim, B. Y.; Kim, S. J.; Lee, C.; Cho, S.; Ko, J.; Kang, S. O. *Organometallics* **2002**, *21*, 1443.
- (26) (a) Glendening, E. D.; Reed, A. E.; Carpenter, J. E.; Weinhold, F. NBO, version 3.1; Theoretical Chemistry Institute and Department of Chemistry, University of Wisconsin, Wisconsin (from <http://www.ccl.net/cca/software/MS-WIN95-NT/mopac6/nbo.htm>). (b) Foster, J. P.; Weinhold, F. *J. Am. Chem. Soc.* **1980**, *102*, 7211.
- (27) Herberhold, M.; Yan, H.; Milius, W.; Wrackmeyer, B. *Z. Anorg. Allg. Chem.* **2000**, *626*, 1627.
- (28) (a) Zakharkin, L. I.; Kovredov, A. I.; Olshevskaya, V. A.; Antonovich, V. A. *J. Organomet. Chem.* **1984**, *267*, 81. (b) Aldridge, S.; Kays, D. L.; Al-Fawaz, A.; Jones, K. M.; Horton, P. N.; Hursthouse, M. B.; Harrington, R. W.; Clegg, W. *Chem. Commun.* **2006**, 2578.
- (29) (a) Mkhaliid, I. A. I.; Barnard, J. H.; Marder, T. B.; Murphy, J. M.; Hartwig, J. F. *Chem. Rev.* **2010**, *110*, 890. (b) Wei, C. S.; Jimenez-Hoyos, C. A.; Videa, M. F.; Hartwig, J. F.; Hall, M. B. *J. Am. Chem. Soc.* **2010**, *132*, 3078. (c) Wan, X. H.; Wang, X. J.; Luo, Y.; Takami, S.; Kubo, M.; Miyamoto, A. *Organometallics* **2002**, *21*, 3703.
- (30) (a) Wang, X. T.; Sabat, M.; Grimes, R. N. *J. Am. Chem. Soc.* **1995**, *117*, 12227. (b) Weinmann, W.; Wolf, A.; Pritzkow, H.; Siebert, W.; Barnum, B. A.; Carroll, P. J.; Sneddon, L. G. *Organometallics* **1995**, *14*, 1911. (c) Ilkhechi, A. H.; Scheibitz, M.; Bolte, M.; Lerner, H. W.; Wagner, M. *Polyhedron* **2004**, *23*, 2597. (d) Glockner, A.; Daniliuc, C. G.; Freytag, M.; Jones, P. G.; Tamm, M. *Chem. Commun.* **2012**, *48*, 6598.
- (31) (a) Bachrach, S. M. *J. Org. Chem.* **1993**, *58*, 5414. (b) Kunitada, T.; Omatsu, R.; Tanaka, N.; Imai, N.; Inokuchi, T.; Nokami, J. *Tetrahedron Lett.* **2010**, *51*, 5525.
- (32) Mihailovic, M. L.; Milosavljevic, S.; Jeremic, D.; Milovanovic, J. *Org. Magn. Reson.* **1977**, *9*, 229.
- (33) (a) Rajsekhar, G.; Rao, C. P.; Saarenketo, P. K.; Kolehmainen, E.; Rissanen, K. *Inorg. Chem. Commun.* **2002**, *5*, 649. (b) Singh, A. K.;

Mukherjee, R. *Dalton Trans.* **2008**, 260. (c) Wang, L. D.; He, W.; Yu, Z. K. *Chem. Soc. Rev.* **2013**, 42, 599.

(34) For carboranyl C–S cleavage: Teixidor, F.; Pedrajas, J.; Vinas, C. *Inorg. Chem.* **1995**, 34, 1726. Examples for carboranyl C–Se cleavage: (a) Wrackmeyer, B.; Hernandez, Z. G.; Kempe, R.; Herberhold, M. Z. *Anorg. Allg. Chem.* **2007**, 633, 851. (b) Wrackmeyer, B.; Hernandez, Z. G.; Kempe, R.; Herberhold, M. *Appl. Organomet. Chem.* **2007**, 21, 108.

(35) Houmam, A. *Chem. Rev.* **2008**, 108, 2180.

(36) (a) Bott, S. G.; Marchand, A. P.; Kumar, K. A. *J. Chem. Crystallogr.* **1996**, 26, 281. (b) Taffin, C.; Kreutler, G.; Bourgeois, D.; Clot, E.; Perigauda, C. *New J. Chem.* **2010**, 34, 517.

(37) (a) Grosclaude, J. P.; Gonzenbach, H. U.; Perlberger, J. C.; Schaffner, K. *J. Am. Chem. Soc.* **1975**, 97, 4147. (b) Berson, J. A.; Remanick, A. *J. Am. Chem. Soc.* **1961**, 83, 4947. (c) Berson, J. A.; Reynolds, R. D.; Jones, W. M. *J. Am. Chem. Soc.* **1956**, 78, 6049.

(38) (a) Burgess, K. L.; Lajkiewicz, N. J.; Sanyal, A.; Yan, W. L.; Snyder, J. K. *Org. Lett.* **2005**, 7, 31. (b) Jones, S.; Valette, D. *Org. Lett.* **2009**, 11, 5358. (c) Bula, R. P.; Oppel, I. M.; Bettinger, H. F. *J. Org. Chem.* **2012**, 77, 3538.

(39) (a) Wu, C.; Xu, B.; Zhao, J.; Jiang, Q.; Wei, F.; Jiang, H.; Wang, X.; Yan, H. *Chem.—Eur. J.* **2010**, 16, 8914. (b) Wu, C.; Ye, H.; Bai, W.; Li, Q.; Guo, D.; Lv, G.; Yan, H.; Wang, X. *Bioconjugate Chem.* **2011**, 22, 16.

(40) Obrecht, D.; Zumbunn, C.; Muller, K. *J. Org. Chem.* **1999**, 64, 6182.

(41) (a) Grieco, P. A.; Abood, N. *J. Org. Chem.* **1989**, 54, 6008. (b) Davies, H. M. L.; Dai, X. *J. Org. Chem.* **2005**, 70, 6680.